Available online at www.sciencedirect.com
SCIENCE DIRECT®
PERGAMON
Polyhedron 22 (2003) 153–163
POLYHEDRON
www.elsevier.com/locate/poly

Neutral and anionic transition metal complexes supported by decafluorodiphenylamido ligands: X-ray crystal structures of $\{Na(THF)_2\}\{Ti[N(C_6F_5)_2]_4\}$, $\{K(\eta^6\text{-}C_6H_5Me)_2\}\{ZrCl_2[N(C_6F_5)_2]_3\}$, $K\{VCl[N(C_6F_5)_2]_3\}$, $Fe[N(C_6F_5)_2]_2(THF)_2$ and $Co[N(C_6F_5)_2]_2(py)_2$

Garth R. Giesbrecht [a], John C. Gordon [b,*], David L. Clark [a,*], Cybele A. Hijar [b], Brian L. Scott [b], John G. Watkin [b,*]

[a] *Nuclear Materials Technology (NMT) Division and Glenn T. Seaborg Institute for Transactinium Science, Los Alamos National Laboratory, Los Alamos, NM 87545, USA*

[b] *Chemistry (C) Division, Los Alamos National Laboratory, Los Alamos, NM 87545, USA*

Received 23 July 2002; accepted 1 October 2002

Abstract

Reaction of $MN(C_6F_5)_2$ (M = Na, K) with transition metal halides results in the formation of transition metal complexes incorporating decafluorodiphenylamido ligands. $TiCl_3(THF)_3$ reacts with 3 equiv. $NaN(C_6F_5)_2$ to yield the 'metallate' complex $\{Na(THF)_2\}\{Ti[N(C_6F_5)_2]_4\}$ (**1**). Single crystal X-ray diffraction studies reveal a tetrahedral titanium center complexed by four decafluorodiphenylamido ligands; while two THF ligands and four fluorine atoms coordinate the sodium cation. $ZrCl_4$ reacts with 3 equiv. $KN(C_6F_5)_2$ to give $\{K(\eta^6\text{-}C_7H_8)_2\}\{ZrCl_2[N(C_6F_5)_2]_3\}$ (**2**). The ^{19}F NMR spectrum of **2** reveals phenyl resonances in a 2:1 ratio, consistent with a trigonal bipyramidal structure being maintained in solution. The crystal structure of **2** reveals a pseudo-octahedral structure, with the sixth-coordination site being completed by a weak Zr–F interaction with a pentafluorophenyl group of an amido ligand. The potassium counterion interacts in an η^6 fashion with two toluene rings in addition to a fluorine atom arising from one of the pentafluorophenyl groups. The reaction of VCl_3 with 3 equiv. $KN(C_6F_5)_2$ generates the 'metallate' complex $K\{VCl[N(C_6F_5)_2]_3\}$ (**3**); the solid state structure of **3** reveals a distorted trigonal bipyramid with the coordination sphere being completed by a weak V–F interaction with the *ortho*-fluorine of one of the fluorophenyl amido ligands. Exposure of $FeCl_3$ to 3 equiv. $KN(C_6F_5)_2$ results in reduction of the metal center and the formation of the Fe(II) species $Fe[N(C_6F_5)_2]_2(THF)_2$ (**4**). Compound **4** is tetrahedral in the solid state with none of the weak M–F contacts observed for **1**, **2**, **3** and **5**. CoI_2 reacts with 2 equiv. $NaN(C_6F_5)_2$ in the presence of pyridine to produce the expected product $Co[N(C_6F_5)_2]_2(py)_2$ (**5**); X-ray crystallography reveals a five-coordinate species in the solid state which is additionally stabilized by a weak Co–F interaction.

Keywords: Decafluorodiphenylamido; Titanium; Zirconium; Vanadium; Iron; Cobalt

1. Introduction

The chemistry of transition metals coordinated by amido ligands has grown dramatically in the past decade, due in part to the realization that the amido ligand may be an attractive alternative to the cyclopentadienyl ligand as a result of the ease with which electronic and steric changes may be incorporated into the ligand framework [1–4]. The chemistry of transition-metal amido complexes has been greatly accelerated by the observation of catalytic activity [5–11] and small molecule activation [12,13]. Although a number of studies have utilized pentafluorophenyl groups attached to the nitrogen atom of amido ligands, [14–21] there have been no reports to date of the use of the decafluorodiphenylamido group, $-N(C_6F_5)_2$, as an ancillary ligand in transition metal complexes. We were interested in the decafluorodiphenylamido ligand

* Corresponding authors. Tel.: +1-505-665-6690; fax: +1-505-665-7895
E-mail address: dlclark@lanl.gov (D.L. Clark).

0277-5387/02/$ - see front matter
PII: S0277-5387(02)01258-5

due to its facile synthesis [22], its high solubility in hydrocarbon solvents, and its suitable steric requirements. The electron withdrawing nature of this ligand may be understood by considering the pK_a of the amine, which has been determined to be very similar to those of trifluoroacetic acid and pentafluorobenzoic acid [23]. Studies of pK_a values of a range of amines in various solvents revealed that the pK_a of aniline in DMSO is 30.6, diphenylamine is 25.0 and decafluorodiphenylamine is 11.5 [24]. This suggested that the decafluorodiphenylamido ligand may be helpful in stabilizing highly electrophilic metal amido complexes as potential catalysts for olefin polymerization [25]. Recently, we reported the use of this ligand in organolanthanide chemistry, which resulted in the isolation of the unusual toluene complex, (η^6-C_7H_8)Nd[$N(C_6F_5)_2$]$_3$ [26]. Here we report the synthesis and crystallographic characterization of transition metal centers supported by the highly electron-withdrawing $-N(C_6F_5)_2$ ligand.

2. Results and discussion

2.1. Synthesis

The reaction of either $NaN(C_6F_5)_2$ or $KN(C_6F_5)_2$, generated in situ by the reaction of NaH or KH with $HN(C_6F_5)_2$ in THF, with transition metal chlorides resulted in the formation of new transition metal complexes containing decafluorodiphenylamido ligands (Eqs. (1)–(5)).

$$3NaN(C_6F_5)_2 + TiCl_3(THF)_3 \xrightarrow[RT,\ 18\ h]{THF/tol} \{Na(THF)_2\}\{\underset{\mathbf{1}}{Ti[N(C_6F_5)_2]_4}\} \quad (1)$$

$$3KN(C_6F_5)_2 + ZrCl_4 \xrightarrow[RT,\ 18\ h]{THF/tol} \{K(C_7H_8)_2\}\{\underset{\mathbf{2}}{ZrCl_2[N(C_6F_5)_2]_3}\} \quad (2)$$

$$3KN(C_6F_5)_2 + VCl_3 \xrightarrow[RT,\ 18\ h]{THF/tol} K\{\underset{\mathbf{3}}{VCl[N(C_6F_5)_2]_3}\} \quad (3)$$

$$3KN(C_6F_5)_2 + FeCl_3 \xrightarrow[RT,\ 18\ h]{THF/tol} \underset{\mathbf{4}}{Fe[N(C_6F_5)_2]_2(THF)_2} \quad (4)$$

$$2NaN(C_6F_5)_2 + CoI_2 \xrightarrow[RT,\ 18\ h]{THF/tol/pyridine} \underset{\mathbf{5}}{Co[N(C_6F_5)_2]_2(py)_2} \quad (5)$$

In the case of titanium, zirconium and vanadium, various equivalents of amido ligand were incorporated, and the products included sodium or potassium centers, giving anionic or 'metallate' species. The reaction of $NaN(C_6F_5)_2$ (3 equiv.) with $TiCl_3(THF)_3$ gave the blue/green Ti(III) product, $\{Na(THF)_2\}\{Ti[N(C_6F_5)_2]_4\}$ (**1**) in low yield, in which each titanium center was bound to four amido ligands. The titanium atom remained in the +3 oxidation state, with the charge being balanced by a $\{Na(THF)_2^+\}$ counterion. The ^{1}H NMR spectrum of crystalline material exhibited broad peaks due to free THF only; no resonances were observed in the ^{19}F NMR spectrum of **1**, consistent with the paramagnetism of a d^1 Ti(III) metal center. In contrast, the reaction of $TiCl_3(THF)_3$ with the unfluorinated analogue $LiNPh_2$ yields the Ti(IV) product $[Ti(NPh_2)_4]$, in which the titanium center has been oxidized [27]. To the best of our knowledge, no examples of tri-coordinate Ti(III) complexes supported by diphenylamido ligands have been reported.

The reaction of $KN(C_6F_5)_2$ (3 equiv.) with $ZrCl_4$ or VCl_3 yielded the tris amido products $\{K(C_7H_8)_2\}$-$\{ZrCl_2[N(C_6F_5)_2]_3\}$ (**2**) and $K\{VCl[N(C_6F_5)_2]_3\}$ (**3**), both of which additionally coordinated an equivalent of KCl. $\{K(C_7H_8)_2\}\{ZrCl_2[N(C_6F_5)_2]_3\}$ (**2**) was produced as a colorless, diamagnetic solid in moderate yield. The reaction of $ZrCl_4$ with various equivalents of $KN(C_6F_5)_2$ all generated the same product, indicating that **2** is the preferred reaction product. This is in contrast to the reaction of $KNPh_2(dioxane)_3$ with $ZrCl_4(THF)_2$, which produces the tetrakis-amido complex $Zr(NPh_2)_4(dioxane)$ regardless of the stoichiometry employed [28]. The ^{19}F NMR spectrum of **2** was consistent with a trigonal bipyramidal structure being maintained in solution (see later), with two sets of pentafluorophenyl resonances observed in a 2:1 ratio. Based on steric considerations, this is suggestive that two of the decafluorodiphenylamido ligands reside in the equatorial positions, with the remaining ligand occupying an axial position. The ^{1}H NMR spectrum (C_6D_6) of **2** exhibited resonances attributable to free toluene only, suggesting that the $\{K(\eta^6\text{-}C_7H_8)_2^+\}$ unit observed in the solid-state structure may not be maintained in solution (see later), or that the arene unit has exchanged with the NMR solvent. The presence of only two distinct types of phenyl resonances in the ^{19}F NMR spectrum of **2** also suggests that the metal–fluorine interactions observed in the crystal structures of **2**, **3** and **5** are weak and do not give rise to any additional anisotropy in solution.

The formation of the vanadium 'metallate' species also contrasts with that reported for the unfluorinated analogue, for which syntheses of $V(NPh_2)_3(THF)$ [29] $V(NPh_2)_3(THF)(dioxane)_{0.5}$ [30] and $V(NPh_2)_3$ [31] have been reported from the reaction of $VCl_3(THF)_3$ with 3 equiv. of the unsubstituted salt $NaNPh_2$. The mechanism of the reaction of VCl_3 with $KNPh_2$ has been shown to involve the intermediate formation of $K[V(NPh_2)_4]$ [32] showing that the 'metallate' species are also accessible with the less electron withdrawing $-NPh_2$ ligand. $K\{VCl[N(C_6F_5)_2]_3\}$ (**3**) was produced as a dark red solid in low yield. $FeCl_3$ reacted with 3 equiv. of $KN(C_6F_5)_2$ to produce the purple/brown Fe(II) species $Fe[N(C_6F_5)_2]_2(THF)_2$ (**4**) in moderate yield, in which only two decafluorodiphenylamido ligands were evident. By comparison, the reaction of $FeCl_3$ with 3 equiv. of $KNPh_2(dioxane)_3$ in THF produces the metallate

species $K[Fe(NPh_2)_4]$, [33] in which the metal center has not undergone reduction. Similarly, the reaction of $FeBr_2$ with stoichiometric amounts of $MNPh_2(dioxane)_x$ ($M = Li$, $x = 0$; $M = K$, $x = 3$) yields the expected disubstituted Fe(II) products $[Fe(NPh_2)_2]_2$ [34] and $Fe(NPh_2)_2(dioxane)_2$ [34]. The ^1H NMR spectrum of **4** exhibited resonances for free THF only; no resonances were observed in the ^{19}F NMR spectrum, consistent with the presence of a paramagnetic of Fe(II) center.

The reaction of $NaN(C_6F_5)_2$ (2 equiv.) with CoI_2 followed by recrystallisation from toluene–pyridine yielded the expected product, $Co[N(C_6F_5)_2]_2(py)_2$ (**5**) in moderate yield as dark red crystals. Although $CoCl_2$ reacts with 2 equiv. of the unsubstituted salt $LiNPh_2$ to produce a mixture of $[Li(THF)_4][Co(NPh_2)_3]$ and $[Co(NPh_2)_2]_2$ [35] use of the larger halide $CoBr_2$ gives $Co(NPh_2)_2(dioxane)_2$ when reacted with $KNPh_2(dioxane)_3$ in THF [36]. As observed for the titanium complex **1** and the iron species **4**, the paramagnetism of $Co[N(C_6F_5)_2]_2(py)_2$ (**5**) rendered the ^{19}F NMR spectrum uninformative, while only resonances for free solvent were evident by ^1H NMR spectroscopy.

2.2. Crystallographic studies

The above mentioned transition metal complexes **1**–**5** were further investigated by X-ray crystallography in order to establish the nature of the metal–ligand interactions present.

2.2.1. $\{Na(THF)_2\}\{Ti[N(C_6F_5)_2]_4\}$ (**1**)

Single crystals of **1** that were suitable for an X-ray diffraction study were grown by cooling a concentrated toluene solution to −35 °C. Selected bond lengths and angles are presented in Table 1. A thermal ellipsoid plot giving the atom-numbering scheme used in the tables is shown in Fig. 1; complete details of the structural analyses of compounds **1**–**5** are listed in Table 6. Compound **1** co-crystallizes with a molecule of toluene in the unit cell. The titanium metal center is coordinated in pseudo-tetrahedral fashion by four decafluorodiphenylamido ligands, while the sodium cation is bound to two THF ligands and completes its coordination sphere by making short Na–F interactions with four fluorine atoms from four different pentafluorophenyl moieties. The two independent Ti–N bond lengths are identical at 2.039(3) Å, which may be compared with the average distances of 2.089(3) Å seen in the Ti(III) complex $Ti[(2\text{-}(Me_3SiN)\text{-}4\text{-}Me\text{-}C_5H_3N]_3$, [37] 2.035(7)–2.041(7) Å in $[Na(12\text{-crown-}4)_2][\{(Me_3Si)_2N\}_2TiOC(CH_2)SiMe_2NSiMe_3]$, [38] 2.007(7)–2.042(7) in $[Li(12\text{-crown-}4)\{(Me_3Si)_2N\}_2TiCH_2SiMe_2NSiMe_3]$, [39] and 2.027(8) and 2.036(8) Å in $\{Li(TMEDA)_2\}\{Ti[N(SiMe_3)_2]_2(CH_2Ph)_2\}$ [40]. The Na–F distances of 2.407(3) and 2.477(3) Å are entirely in line with those observed previously in many examples of alkali-metal–fluorine interactions [41]. The closest approach of a fluorine atom to the titanium metal center is 3.094 Å in the case of F(1). The Na–O distance of 2.246(4) Å is also unremarkable. Coordination of the sodium cation into the 'pocket' formed by F(11), F(16), F(11*) and F(16*) seems to have little effect on the conformation of the two decafluorodiphenylamido ligands involved in this bonding (i.e. those containing N(2) and N(2*)). In fact, an essentially identical, although vacant, 'pocket' exists at the opposite face of the molecule, formed by F(1), F(6), F(1*) and F(6*). The similarity between the N(2)–Ti(1)–N(2*) angle (115.41(19)°) and the N(1)–Ti(1)–N(1*) angle (123.81(19)°) also indicates that coordination of the sodium cation does not dramatically affect the spatial orientation of the fluorinated ligands. The dihedral angle between the two aromatic rings on each decafluorodiphenylamido ligand is close to 90°, while some of the aromatic rings on adjacent ligands are almost coplanar (e.g. the C(1)–C(6) ring is coplanar to within 1° with the C(19*)–C(24*) ring). Within the extended lattice structure, one can observe two distinct alternating layers-one 'ionic' layer which contains only the titanium, sodium and oxygen atoms, and a 'covalent' layer containing only fluorine and carbon atoms.

Table 1
Selected bond distances (Å) and angles (°) for $\{Na(THF)_2\}\{Ti[N(C_6F_5)_2]_4\}$ (**1**)

Bond lengths			
Ti(1)–N(1)	2.039(3)	Ti(1)–N(2)	2.039(3)
Na(1)–F(11)	2.477(3)	Na(1)–F(16)	2.407(3)
Na(1)–O(1)	2.246(4)	Ti(1)–F(1)	3.094(3)
Bond angles			
N(1)–Ti(1)–N(1*)	123.81(19)	N(1)–Ti(1)–N(2)	117.21(13)
N(1)–Ti(1)–N(2*)	92.63(13)	N(2)–Ti(1)–N(2*)	115.41(19)
O(1)–Na(1)–O(1*)	96.1(3)	O(1)–Na(1)–F(11)	128.53(12)
O(1)–Na(1)–F(16)	151.27(12)	O(1)–Na(1)–F(11*)	82.87(12)
O(1)–Na(1)–F(16*)	95.78(13)	F(11)–Na(1)–F(11*)	136.20(16)
F(11)–Na(1)–F(16)	78.92(10)	F(11*)–Na(1)–F(16)	69.31(9)
F(16)–Na(1)–F(16*)	86.03(14)	Na(1)–F(11)–C(14)	145.1(2)
Na(1)–F(16)–C(20)	124.5(2)		

2.2.2. $\{K(C_7H_8)_2\}\{ZrCl_2[N(C_6F_5)_2]_3\}$ (**2**)

Single crystals of **2** were grown from a concentrated toluene solution at −35 °C; selected bond lengths and angles are presented in Table 2. A thermal ellipsoid plot giving the atom-numbering scheme used in the tables is shown in Fig. 2. The complex crystallizes with one molecule of toluene in the unit cell. The zirconium metal center is coordinated in pseudo-octahedral fashion by two *cis* chloride ligands, three nitrogen atoms from the decafluorodiphenylamido ligands that define a *fac* geometry, and a short Zr···F interaction that lies *trans* to one of the nitrogen atoms. The potassium cation makes one K···F interaction with a fluorine atom from one pentafluorophenyl moiety, and an extended struc-

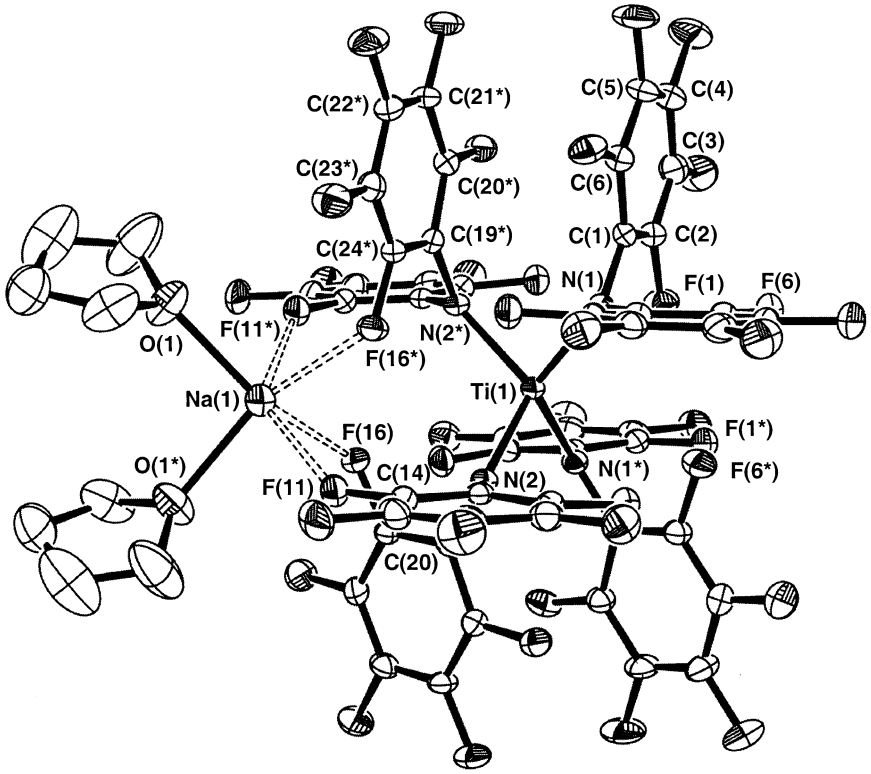

Fig. 1. A thermal ellipsoid view of $\{Na(THF)_2\}\{Ti[N(C_6F_5)_2]_4\}$ (**1**) drawn with 30% probability ellipsoids, and giving the atom number scheme used in the tables. The interstitial toluene molecule is omitted for clarity.

Table 2
Selected bond distances (Å) and angles (°) for $\{K(C_7H_8)_2\}\{ZrCl_2[N(C_6F_5)_2]_3\}$ (**2**)

Bond lengths			
Zr(1)–N(1)	2.102(2)	Zr(1)–N(2)	2.179(2)
Zr(1)–N(3)	2.156(2)	Zr(1)–Cl(1)	2.4882(8)
Zr(1)–Cl(2)	2.4468(8)	Zr(1)–F(26)	2.602(2)
K(1)*–Cl(1)	3.0946(11)	K(1)*–Cl(2)	3.0953(12)
K(1)–F(8)	2.892(2)	K(1)–C(37)	3.247(4)
K(1)–C(38)	3.343(4)	K(1)–C(39)	3.348(5)
K(1)–C(40)	3.258(5)	K(1)–C(41)	3.160(4)
K(1)–C(42)	3.154(4)	K(1)–C(44)	3.203(4)
K(1)–C(45)	3.224(4)	K(1)–C(46)	3.345(6)
K(1)–C(47)	3.453(6)	K(1)–C(48)	3.439(5)
K(1)–C(49)	3.313(4)		
Bond angles			
N(1)–Zr(1)–N(2)	108.64(9)	N(1)–Zr(1)–N(3)	110.55(9)
N(2)–Zr(1)–N(3)	86.18(9)	N(1)–Zr(1)–Cl(1)	91.66(7)
N(2)–Zr(1)–Cl(1)	89.66(6)	N(3)–Zr(1)–Cl(1)	86.88(6)
N(1)–Zr(1)–Cl(2)	101.38(7)	N(2)–Zr(1)–Cl(2)	159.70(7)
N(3)–Zr(1)–Cl(2)	147.44(6)	Cl(1)–Zr(1)–Cl(2)	85.99(3)
N(1)–Zr(1)–F(26)	171.32(8)	N(2)–Zr(1)–F(26)	79.96(8)
N(3)–Zr(1)–F(26)	68.04(7)	Cl(2)–Zr(1)–F(26)	79.42(4)
Cl(1)–Zr(1)–F(26)	79.75(5)	K(1)–F(8)–C(10)	136.9(2)
Zr(1)–F(26)–C(32)	107.10(15)		

ture is then formed by means of K···Cl interactions between the potassium and two zirconium-bound chloride ligands from the adjacent anion in the lattice. Two η^6-toluene solvent molecules also occupy the coordination sphere of potassium. The preference of the potassium cation to interact with two arene rings in a multihapto fashion, despite the fact that the preparative reactions were carried out in a donor solvent (THF) is noteworthy, but not unexpected. The attractive electrostatic interactions of alkali cation-π complexes has been a topic of much recent synthetic and theoretical study [42–47].

The largest deviations of the angles around zirconium from octahedral geometry are the rather obtuse N(1)–Zr(1)–N(3) and N(1)–Zr(1)–N(2) angles of 110.55(9)° and 108.64(9)°, respectively, and the relatively acute N(3)–Zr(1)–F(26) angle of 68.04(7)°. Zr–N distances are of two types; a relatively short Zr(1)–N(1) distance of 2.102(2) Å and significantly longer Zr(1)–N(2) and Zr(1)–N(3) distances of 2.156(2) and 2.179(2) Å. We note that the short Zr–N bond length occurs in the site that is *trans* to the weak Zr···F interaction, and therefore, suggest that the shortness of the Zr(1)–N(1) bond is due to the virtual absence of a *trans*-influence, when compared with the other two amido ligands which are both *trans* to chloride ligands. The two Zr–Cl bond lengths are very similar, at 2.4468(8) and 2.4882(8) Å, while the Zr(1)–F(26) interaction is 2.6021(17) Å. Only a few other examples of Zr···F interactions are reported in the literature, mainly for weakly coordinating fluorinated anions interacting with cationic zirconium metal centers. For example, Marks et al. noted Zr···F contacts

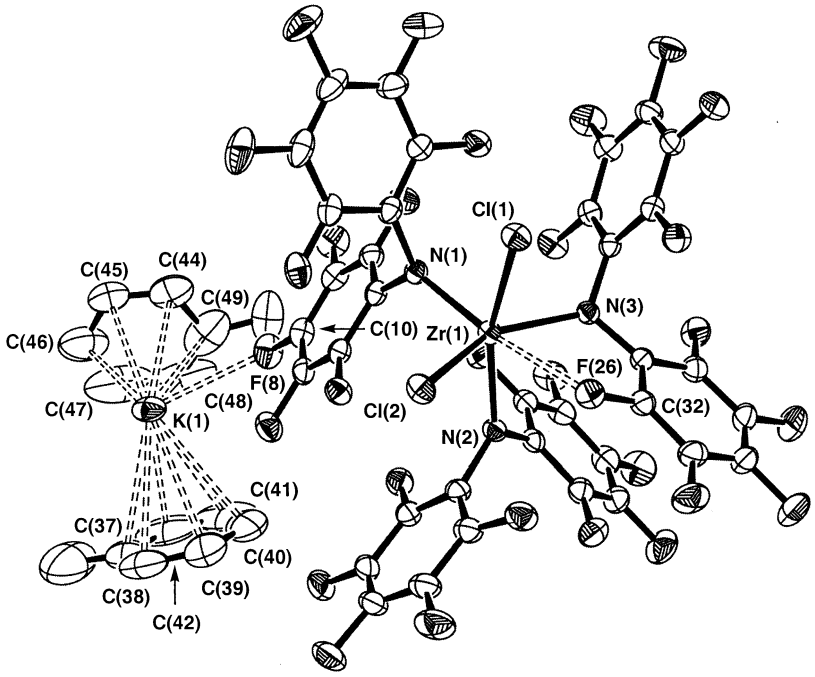

Fig. 2. A thermal ellipsoid view of $\{K(C_7H_8)_2\}\{ZrCl_2[N(C_6F_5)_2]_3\}$ (**2**) drawn with 30% probability ellipsoids, and giving the atom number scheme used in the tables. The interstitial toluene molecule is omitted for clarity.

of 2.416(3) and 2.534(3) Å in $[(\eta\text{-}C_5Me_5)_2ZrH][HB(C_6F_5)_3]$ [48,49] while Gade and co-workers have reported Zr···F distances of 2.535(5) Å in $[(2\text{-}FC_6H_4NSiMe_2)_3CH]Zr(\mu\text{-}Cl)_2Li(OEt)_2$ [50] and 2.563(8) Å in $HC[SiMe_2N(2\text{-}FC_6H_4)]_3Zr(S_2C)Fe(CO)_2(\eta\text{-}C_5H_5)$ [51]. Also Erker has observed Zr···F distances of 2.408(2) Å in $(\eta\text{-}C_5H_4Me)_2Zr[H_2CCHCHCH_2B(C_6F_5)_3]$ [52] and 2.4020(13) Å in $(\eta\text{-}C_5H_5)_2Zr[H_2CC(Me)CHCH_2B(C_6F_5)_3]$ [52] and a Zr···F distance as short as 2.237(4) Å has been documented in $\{(\eta\text{-}C_5Me_5)[\eta\text{-}C_5Me_4CH_2B(C_6F_5)_3]ZrH\}$ [53]. The Zr–Cl distances are comparable to those of 2.475(3) Å seen in $\{C_6H_5C[N(SiMe_3)][(N(myrtanyl)\}_3ZrCl$ and 2.4231(11) Å in $ZrCl\{N[CH_2CH_2N(SiMe_2Bu^t)]_3\}$ [54]. K–Cl distances of 3.0953(12) and 3.0946(11) Å are slightly shorter than those observed in crystalline KCl (3.138 Å) [55] while the K(1)–F(8) distance of 2.892(2) Å is typical for interactions of this type [41]. K–C distances for the η^6-bound toluene molecules lie in the range 3.154(4)–3.453(6) Å, which may be compared with those found in $[Lu\{CH(SiMe_3)_2\}_3(\mu\text{-}Cl)K(\eta^6\text{-}toluene)_2]$ (3.21–3.56 Å) [56] $[(Tmp)_6Sm_2(KCl)_2(toluene)_3]_n$ (Tmp = 2,3,4,5-tetramethylphospholyl; 3.21–3.56 Å) [57] and $[\{(Bu^tO)_2Sb_3(\mu\text{-}NCy)_3(\mu_3\text{-}NCy)\}K(\eta^6\text{-}toluene)]$ (3.20–3.47 Å) [58].

2.2.3. $K\{VCl[N(C_6F_5)_2]_3\}$ (3)

Cooling a concentrated 3:1 toluene–hexane solution to −35 °C grew single crystals of **3** that were suitable for X-ray diffraction. A list of relevant bond lengths and angles is presented in Table 3; a thermal ellipsoid view is shown in Fig. 3. Compound **3** co-crystallizes with one molecule of toluene per unit cell. The overall molecular geometry consists of a vanadium metal center coordinated in a distorted trigonal bipyramidal fashion by an axial chloride ligand, an axial V···F–C interaction with the *ortho*-fluorine of one of the amido ligands, and three decafluorodiphenylamido ligands which occupy meridianal positions. The chain structure of this complex, formed by means of K···Cl···K···Cl bridges is reminiscent of that seen in $\{Th[Me_3SiCHC(Bu^t)NSiMe_3)]_2(\mu_3\text{-}Cl)(\mu\text{-}Cl)_2K(OEt_2)\}_n$ [59]. The N–V–N angles within the equatorial plane are all roughly 120°, while the axial Cl(1)–V(1)–F(12) angle measures 172.85(6)°. The vanadium–nitrogen distances of 1.944(3), 1.991(3) and 2.000(3) Å span the range of

Table 3
Selected bond distances (Å) and angles (°) for $K\{VCl[N(C_6F_5)_2]_3\}$ (**3**)

Bond lengths			
V(1)–N(1)	1.991(3)	V(1)–N(2)	1.944(3)
V(1)–N(3)	2.000(3)	V(1)–Cl(1)	2.2999(12)
V(1)–F(12)	2.284(2)	K(1)–F(2)	2.727(3)
K(1)–F(30)	2.739(3)	K(1)–F(32)	2.873(3)
K(1)–Cl(1)	3.0925(14)		
Bond angles			
N(1)–V(1)–N(2)	114.63(13)	N(1)–V(1)–N(3)	111.53(13)
N(1)–V(1)–Cl(1)	97.56(10)	N(1)–V(1)–F(12)	76.83(10)
N(2)–V(1)–N(3)	130.01(13)	N(2)–V(1)–Cl(1)	99.64(9)
N(2)–V(1)–F(12)	86.82(10)	N(3)–V(1)–Cl(1)	92.27(9)
N(3)–V(1)–F(12)	85.80(10)	Cl(1)–V(1)–F(12)	172.85(6)
V(1)–F(12)–C(12)	109.3(2)		

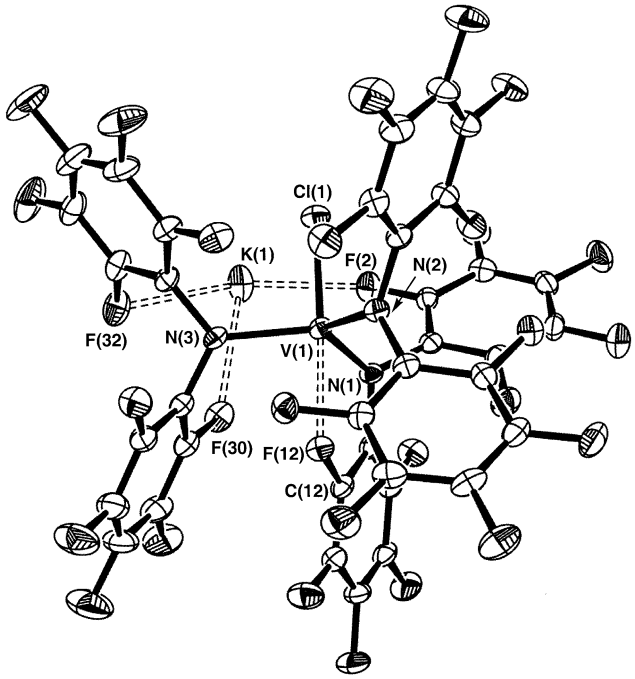

Fig. 3. A thermal ellipsoid view of K{VCl[N(C_6F_5)$_2$]$_3$} (**3**) drawn with 30% probability ellipsoids, and giving the atom number scheme used in the tables; only half of the dimer is shown. The interstitial toluene molecule is omitted for clarity.

those previously reported for similar compounds, i.e. V–N distances of 1.934(2) and 1.988(2) Å were observed in V[N($SiMe_3$)$_2$]$_2$Ph(py) [60] 1.950(3) Å (ave.) in [(Me_3-Si)$_2$N]$_2$V(*o*-$Me_2NCH_2C_6H_4$) [60] 1.937(2)–1.961(2) Å in V(NPh_2)$_3$(THF) [29] 1.988(7)–2.004(7) Å in [Li(THF)$_4$][V(NPh_2)$_4$] [61] and 1.94(2) Å in [(Me_3-Si)$_2$N]N[N($SiMe_3$)$SiMe_2CH_2$](py) [62]. The V–Cl distance of 2.2999(12) Å is similar to those observed in {Li(TMEDA)$_2$}{VCl$_2$[N($SiMe_3$)$_2$]$_2$} (2.309(1) and 2.311(1) Å), [63] (Ph_2nacnac)VCl$_2$(THF)$_2$ (2.362 Å) [64] and {$NHEt_3$}{VCl$_2$[C_6H_4-1,2-(NHCO-2-C_5H_4N)$_2$} (2.350(1) and 2.357(1) Å) [65]. The only significant vanadium–fluorine contact in **3** is the V(1)···F(12) interaction of 2.284(2) Å, which may be compared with that of 2.306(2) and 2.378(2) Å in VCl[2,4,6-(CF_3)$_3C_6H_2$]$_2$(THF) [66]. K···Cl interactions of 3.0925(14) Å are similar to those of 3.269–3.288 Å in [K(18-crown-6)]$_2$[$SeCl_6$] [67] 2.618(7) and 2.938(9) Å in {Th[$Me_3SiCHC(Bu^t)NSiMe_3$)]$_2$(μ_3-Cl)(μ-Cl)$_2$K(OEt_2)}$_n$ [59] and the intermolecular K···Cl distances of 3.0953(12) and 3.0946(11) Å determined for **2**.

2.2.4. *Fe[N(C_6F_5)$_2$]$_2$(THF)$_2$ (**4**)*

Single crystals of **4** that were amenable to X-ray diffraction were grown from a concentrated toluene solution at −35 °C. A thermal ellipsoid view of the structure is presented in Fig. 4; selected bond lengths and angles are available in Table 4. The iron center sits on a twofold rotation axis, and is coordinated in approximately tetrahedral fashion by two nitrogen atoms from decafluorodiphenylamido ligands and two oxygen atoms from the THF ligands. The angles subtended by iron range from 99.44(7)° (N(1)–Fe(1)–O(1*)) to 132.40(9)° (O(1)–Fe(1)–O(1*)). The Fe–N distance of 2.0495(19) Å is somewhat long for an iron(II)-amido system; distances of ~1.91 Å have been reported for {Fe[N($SiMe_3$)$_2$][μ-*O*-2,4,6-^{t}Bu$_3$-C_6H_2]}$_2$, [68] Fe[N($SiMePh_2$)$_2$]$_2$ [69] and [Fe(μ-NPh_2)(NPh_2)]$_2$ [34]. A Fe–N bond distance of 1.84(2) Å is found in Fe[N($SiMe_3$)$_2$]$_2$ [70]. The Fe–O bond length of 2.1193(16) Å may be compared with the distances of 2.136(4) Å seen in [calix[4](OMe)$_2$(O)$_2$Fe-(THF)], [71] 2.0941(19) Å observed in {Fe$_2$(μ-O_2CAr)$_2$(O_2CAr)$_2$(THF)$_2$}, [72] and 2.071(6) Å seen in Fe[N($SiMe_3$)$_2$]$_2$(THF) [34]. The closest Fe···F distance of 3.409(2) Å (Fe(1)–F(5)) is similar to that of 2.105(3) Å seen for an iron–hexafluoroantimonate interaction in [Fe(TPP)][SbF_6] (TPP = tetraphenylporphinato) [73].

2.2.5. *Co[N(C_6F_5)$_2$]$_2$(py)$_2$ (**5**)*

Cooling a concentrated toluene solution of **5** to −35 °C yielded crystals of the cobalt complex that were suitable for diffraction analysis. A thermal ellipsoid drawing is shown in Fig. 5; relevant bond lengths

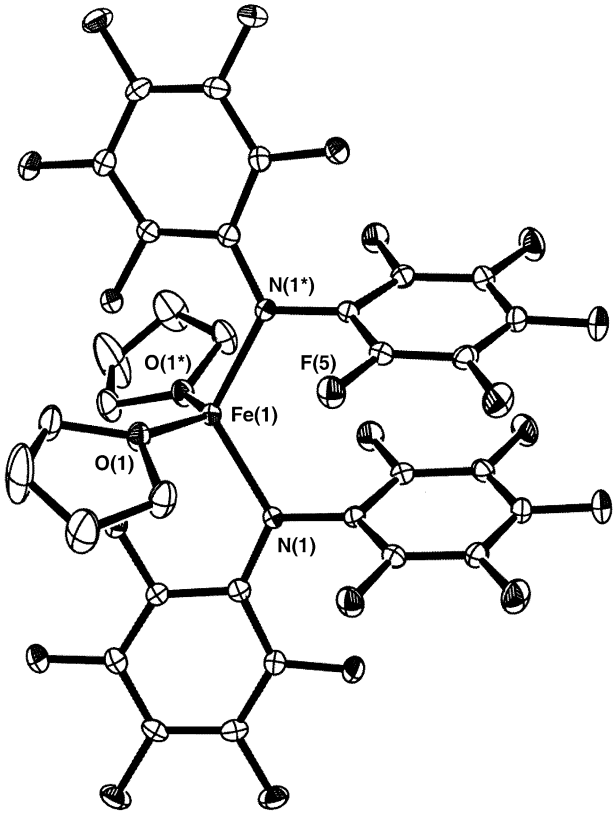

Fig. 4. A thermal ellipsoid view of Fe[N(C_6F_5)$_2$]$_2$(THF)$_2$ (**4**) drawn with 30% probability ellipsoids, and giving the atom number scheme used in the tables.

Table 4
Selected bond distances (Å) and angles (°) for $Fe[N(C_6F_5)_2]_2(THF)_2$ (**4**)

Bond lengths			
Fe(1)–N(1)	2.0495(19)	Fe(1)–O(1)	2.1193(16)
Fe(1)–F(5)	3.409(2)		
Bond angles			
N(1)–Fe(1)–N(1*)	121.19(11)	N(1)–Fe(1)–O(1)	103.43(7)
N(1)–Fe(1)–O(1*)	99.44(7)	O(1)–Fe(1)–O(1*)	132.40(9)

and angles are presented in Table 5. The solid-state structure of **5** includes a molecule of toluene in the crystal lattice. The coordination geometry about the cobalt metal center approximates a trigonal bipyramid, with N(3) and F(8) occupying axial positions, and N(1), N(2) and N(4) in the meridianal plane. The Co–N(pyridine) distances of 2.090(3) and 2.053(3) Å are comparable with those of 2.087(4) and 2.102(5) Å seen in $Co\{[OC(CF_3)_2CH_2]_2S\}(py)_2$ [74]. The Co–N(amide) distances of 1.989(3) and 1.979(3) Å are slightly longer than those observed in $\{Co[N(SiMe_3)_2]_2\}_2$ (1.922(5) and 1.910(5) Å) [75] and $[Co(NPh_2)_2]_2$ (1.889(8) Å) [35]. The Co···F interaction of 2.507(2) Å is longer than the cobalt-hexafluorosilicate Co···F distance of 2.143(2) Å in $[Co(NVI)_4(\mu\text{-}SiF_6)]$ (NVI = *N*-vinylimidazole) [76] but comparable to the Co···F distance of 2.65(2) Å seen in $Co[HB(3,5\text{-}Me_2Pz)_3](C_6F_5)$ [77]. Cotton and co-workers have observed a Co–F distance of 2.223(5) Å between a trinuclear cobalt cation and a tetrafluorobo-

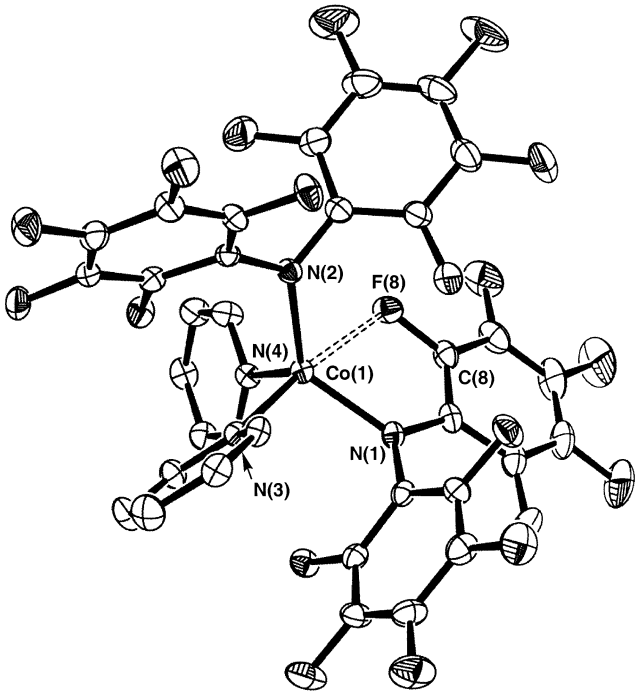

Fig. 5. A thermal ellipsoid view of $Co[N(C_6F_5)_2]_2(py)_2$ (**5**) drawn with 30% probability ellipsoids, and giving the atom number scheme used in the tables. The interstitial toluene molecule is omitted for clarity.

Table 5
Selected bond distances (Å) and angles (°) for $Co[N(C_6F_5)_2]_2(py)_2$ (**5**)

Bond lengths			
Co(1)–N(1)	1.989(3)	Co(1)–N(2)	1.979(3)
Co(1)–N(3)	2.090(3)	Co(1)–N(4)	2.053(3)
Co(1)–F(8)	2.507(2)		
Bond angles			
N(1)–Co(1)–N(2)	127.81(13)	N(1)–Co(1)–N(3)	99.98(12)
N(1)–Co(1)–N(4)	109.94(13)	N(1)–Co(1)–F(8)	73.6(1)
N(2)–Co(1)–N(3)	95.85(12)	N(2)–Co(1)–N(4)	112.13(13)
N(2)–Co(1)–F(8)	87.4(1)	N(3)–Co(1)–N(4)	107.09(12)
N(3)–Co(1)–F(8)	173.4(1)	N(4)–Co(1)–F(8)	76.8(1)
Co(1)–F(8)–C(8)	106.1(2)		

rate anion in $[Co_3(dpa)_4Cl]BF_4$ (dpa = dipyridylamine) [78].

3. Conclusions

We have shown that the decafluorodiphenylamido ligand is easily introduced to a wide variety of transition metals by simple metathetical synthetic procedures. Although early transition metals such as titanium, zirconium and vanadium prefer to form anionic metallate complexes, this tendency is less pronounced for the later transition metals. In the solid state, the decafluorodiphenylamido ligand displays a marked tendency to form secondary interactions between the central metal ion and *ortho*-fluorine atoms on the fluorophenyl substituent. Although numerous examples of secondary M–F interactions were discovered in the solid state, these were not observed in solution, suggesting that such interactions are probably weak and do not occur within the coordination sphere of the metal under normal reaction conditions. Thus, it can be seen that the highly electron-withdrawing decafluorodiphenylamido ligand may be used to support electrophilic transition metal centers; these complexes may prove useful in applications such as olefin polymerization where such requirements are favorable.

4. Experimental

4.1. General considerations

All manipulations were carried out under an inert atmosphere of oxygen-free UHP grade argon using standard Schlenk techniques or under oxygen-free helium in a Vacuum Atmospheres glove box. Decafluorodiphenylamine [22] and $TiCl_3(THF)_3$ [79] were prepared as described previously. $ZrCl_4$ and VCl_3 were purchased from Strem Chemical Co. and used as received. $FeCl_3$ was obtained from Acros and used as received. NaH and CoI_2 were purchased from Aldrich

and used as received. Pyridine was purchased from Aldrich and distilled over sodium prior to use. Toluene, THF and hexanes were de-oxygenated by passage through a column of supported copper redox catalyst (Cu-0226 S) and dried by passing through a second column of activated alumina. C_6D_6 and C_7D_8 were dried over Na–K alloy, trap-to-trap distilled and degassed before use. ^{1}H NMR spectra were recorded on a Varian Unity 300 spectrometer at ambient temperature; ^{1}H chemical shifts are given relative to residual C_6D_5H ($\delta = 7.15$ ppm) or C_7D_7H ($\delta = 2.09$ ppm). ^{19}F NMR spectra were recorded on a Bruker DRX-500 spectrometer at ambient temperature; ^{19}F chemical shifts are given relative to external $CFCl_3$ ($\delta = 0.0$ ppm). Infrared spectra were recorded on a Digilab FTS-40 FT-IR spectrometer; solid-state spectra were taken as Nujol mulls between KBr plates, and calibrated against a polyethylene standard. Elemental analyses were performed on a Perkin–Elmer 2400 CHN analyzer. Elemental analysis samples were prepared and sealed in tin capsules in the glove box prior to combustion.

4.1.1. *{Na(THF)$_2$}{Ti[N(C$_6$F$_5$)$_2$]$_4$} (**1**)*

In the dry box, decafluorodiphenylamine (1.00 g, 2.9 mmol) was dissolved in 30 ml of THF and an excess (0.20 g, 8.3 mmol) of sodium hydride was added. The solution was stirred at room temperature (r.t.) for 10 min, until gas evolution had subsided. Stirring was discontinued, and the excess sodium hydride allowed to settle. The supernatant sodium amide solution was removed with a pipette and added to a solution of $TiCl_3(THF)_3$ (0.35 g, 1.0 mmol) in 50 ml of THF. The reaction mixture was allowed to stir at r.t. for 18 h to produce a deep green solution with some white precipitate. All solvent was removed in vacuo to leave a greenish solid. This was washed with hexanes (30 ml) and then extracted with toluene (50 ml). The toluene extract was allowed to stand at r.t., producing large blue/green crystals. These were decanted free from the solution and stored under fresh toluene at −35 °C. The remaining solution was filtered through Celite and the filtrate reduced in volume to 30 ml, at which point, a microcrystalline solid was being deposited. The solution was heated to 50 °C to redissolve the solid, allowed to stand at r.t., and then placed in the freezer. Overnight, blue/green crystals were deposited. The crystals were isolated by decanting the mother liquor and drying in vacuo (0.26 g, 15% yield). ^{1}H NMR (300 MHz, C_6D_6): only resonances for free THF were observed. ^{19}F NMR (470 MHz, C_7D_8): due to the paramagnetism of **1**, no ^{19}F resonances were observed. IR (Nujol, cm^{-1}): 1659 (w), 1519 (s), 1366 (m), 1315 (w), 1266 (w), 1168 (w), 1032 (s), 982 (m), 844 (m), 722 (m), 667 (m). *Anal.* Calc. for $C_{48}F_{40}N_4NaTi$ [**1**-2(THF)]: C, 39.40; N, 3.83. Found: C, 37.94; N, 3.75%.

4.1.2. *{K(C$_7$H$_8$)$_2$}{ZrCl$_2$[N(C$_6$F$_5$)$_2$]$_3$} (**2**)*

In the dry box, decafluorodiphenylamine (2.1 g, 6.0 mmol) was dissolved in 30 ml of THF and a slight excess (0.33 g, 8.2 mmol) of potassium hydride was added. The solution was stirred at r.t. for 10 min, until gas evolution had subsided. Stirring was discontinued, and the excess potassium hydride allowed to settle. The supernatant potassium amide solution was removed with a pipette and added to a slurry of $ZrCl_4$ (0.47 g, 2.0 mmol) in 50 ml of THF. The reaction mixture was allowed to stir at r.t. for 18 h and the resulting off-white suspension filtered through a Celite pad. The filtrate was pumped to dryness and the resulting solid was extracted with toluene (100 ml). The solution was again filtered through Celite and the filtrate reduced in volume to 10 ml before being placed in the freezer at −35 °C. Over a period of several days, large colorless crystals were deposited. The crystals were isolated by decanting the mother liquor and allowing the crystals to dry in the dry box atmosphere (1.7 g, 57% yield). ^{1}H NMR (300 MHz, C_6D_6): only resonances for free toluene were observed. ^{19}F NMR (470 MHz, C_7D_8): δ −111.9 (d, $^3J_{F-F} = 22.6$ Hz, 8F, *ortho*-F), −113.0 (d, $^3J_{F-F} = 22.6$ Hz, 4F, *ortho*-F), −124.7 (t, $^3J_{F-F} = 22.6$ Hz, 4F, *para*-F), −126.3 (t, $^3J_{F-F} = 22.6$ Hz, 2F, *para*-F), −128.4 (t, $^3J_{F-F} = 22.6$ Hz, 4F, *meta*-F), −128.5 (t, $^3J_{F-F} = 22.6$ Hz, 8F, *meta*-F). IR (Nujol, cm^{-1}): 1633 (m), 1519 (s), 1303 (m), 1169 (w), 1145 (w), 1032 (s), 824 (w), 727 (s), 694 (m), 613 (m). *Anal.* Calc. for $C_{43}H_8Cl_2F_{30}KN_3Zr$ [**2**-(toluene)]: C, 38.61; H, 0.60; N, 3.14. Found: C, 37.84; H, 0.84; N, 2.98%.

4.1.3. *K{VCl[N(C$_6$F$_5$)$_2$]$_3$} (**3**)*

In the dry box, decafluorodiphenylamine (1.00 g, 2.9 mmol) was dissolved in 30 ml of THF and an excess (0.15 g, 3.7 mmol) of potassium hydride was added. The solution was stirred at r.t. for 10 min, until gas evolution had subsided. Stirring was discontinued, and the excess potassium hydride allowed to settle. The supernatant potassium amide solution was removed with a pipette and added to a slurry of vanadium trichloride (0.150 g, 1.0 mmol) in 50 ml of THF. The reaction mixture was allowed to stir at r.t. for 18 h to produce a deep red solution with some gelatinous precipitate. All solvent was removed in vacuo to leave a dark solid. This was washed with hexanes (30 ml) and then extracted with toluene (50 ml). The extract was filtered through Celite and the filtrate reduced in volume to 10 ml before 3 ml of hexanes was added and the solution was placed in the freezer at −35 °C. Overnight, clumps of very dark red crystals were formed. The crystals were isolated by decanting the mother liquor and then dried in vacuo (0.55 g, 22% yield). ^{19}F NMR (470 MHz, C_7D_8); due to the paramagnetism of **3**, no ^{19}F resonances of the complex were observed. IR (Nujol, cm^{-1}): 1643 (w), 1518 (s), 1306 (m), 1154 (w), 1032 (s), 982 (m), 824 (w),

727 (m), 660 (w). *Anal.* Calc. for $C_{36}ClF_{30}KN_3V$: C, 36.96; N, 3.59. Found: C, 34.99; N, 3.86%.

4.1.4. $Fe[N(C_6F_5)_2]_2(THF)_2$ (**4**)

In the dry box, decafluorodiphenylamine (1.00 g, 2.9 mmol) was dissolved in 30 ml of THF and an excess (0.15 g, 3.7 mmol) of potassium hydride was added. The solution was stirred at r.t. for 10 min, until gas evolution had subsided. Stirring was discontinued, and the excess potassium hydride allowed to settle. The supernatant potassium amide solution was removed with a pipette and added to a solution of $FeCl_3$ (0.15 g, 1.0 mmol) in 50 ml of THF. The reaction mixture was allowed to stir at r.t. for 18 h to produce a deep red/purple solution with some precipitate. All solvent was removed in vacuo to leave a dark solid. This was washed with hexanes (30 ml) and then extracted with toluene (50 ml). The extract was filtered through Celite and the filtrate reduced in volume to 10 ml before 5 ml of hexanes was added and the solution was placed in the freezer at −35 °C. Overnight, pale purple/brown crystals were deposited. The crystals were isolated by decanting the mother liquor and drying in vacuo (0.46 g, 51% yield). ^{1}H NMR (300 MHz, C_6D_6): only resonances for free THF were observed. ^{19}F NMR (470 MHz, C_7D_8): due to the paramagnetism of **4**, no ^{19}F resonances were observed. IR (Nujol, cm^{-1}): 1658 (m), 1519 (s), 1346 (m), 1306 (m), 1268 (m), 1182 (m), 1137 (w), 1032 (s), 982 (s), 828 (m), 727 (m), 695 (m), 675 (w), 648 (w), 605 (w). *Anal.* Calc. for $C_{24}F_{20}FeN_2$ [**4**-2(THF)]: C, 38.33; N, 3.72. Found: C, 37.30; N, 3.51%.

4.1.5. $Co[N(C_6F_5)_2]_2(py)_2$ (**5**)

In the dry box, decafluorodiphenylamine (1.00 g, 2.9 mmol) was dissolved in 30 ml of THF and an excess (0.20 g, 8.3 mmol) of sodium hydride was added. The solution was stirred at r.t. for 10 min, until gas evolution had subsided. Stirring was discontinued, and the excess sodium hydride allowed to settle. The supernatant sodium amide solution was removed with a pipette and added to a solution of CoI_2 (0.45 g, 1.4 mmol) in 50 ml of THF. The reaction mixture was allowed to stir at r.t. for 18 h to produce a deep blue/green solution with some white precipitate. The solution was filtered through Celite, and the filtrate pumped dry to leave a green/red dichroic oil. One milliliter of pyridine was added to the oil, at which point it became blood red. The pyridine was removed in vacuo, and the residue dissolved in toluene (5 ml). This solution was layered with hexanes (5 ml) and placed in the freezer at −35 °C. Very dark red crystals were deposited overnight. The crystals were isolated by decanting the mother liquor and drying briefly in vacuo (0.89 g, 63% yield). ^{1}H NMR (300 MHz, C_6D_6): only resonances for free pyridine were observed. ^{19}F NMR (470 MHz, C_7D_8): due to the paramagnetism of **5**, no ^{19}F resonances were observed. IR (Nujol, cm^{-1}): 1606 (w), 1503 (s), 1306 (w), 1217 (m), 1024 (s), 980 (s), 827 (w), 754 (m), 726 (m), 699 (m), 610 (w). *Anal.* Calc. for $C_{34}H_{10}CoF_{20}N_4$: C, 44.71; H, 1.10; N, 6.13. Found: C, 43.34; H, 1.48; N, 5.80%.

5. Crystallographic studies

The crystal structures of all compounds were determined as follows, with exceptions noted in subsequent paragraphs: a crystal was mounted onto a glass fiber using a spot of silicone grease. Due to air sensitivity, the crystal was mounted from a pool of mineral oil under argon gas flow. The crystal was placed on a Bruker P4/CCD diffractometer, and cooled to 203 K using a Bruker LT-2 temperature device. The instrument was equipped with a sealed, graphite monochromatized Mo Kα X-ray source ($\lambda = 0.71073$ Å). A hemisphere of data was collected using φ-scans, with 30 s frame exposures and 0.3° frame widths. Data collection and initial indexing and cell refinement were handled using SMART [80] software. Frame integration, including Lorentz-polarization corrections, and final cell parameter calculations were carried out using SAINT [81] software. The data were corrected for absorption using the SADABS [82] program. Decay of reflection intensity was monitored via analysis of redundant frames. The structure was solved using Direct methods and difference Fourier techniques. All hydrogen atom positions were idealized, and rode on the atom they were attached to. The final refinement [83] included anisotropic temperature factors on all non-hydrogen atoms. Structure solution, refinement, graphics, and creation of publication materials were performed using SHELXTL NT [84]. Additional details of data collection and structure refinement are listed in Table 6.

5.1. $\{Na(THF)_2\}\{Ti[N(C_6F_5)_2]_4\}$ (**1**)

A disordered lattice toluene was restrained to approximate ideal geometry, and was refined with isotropic thermal parameters. The toluene was disordered on an inversion center, and the methyl group was refined at one-half occupancy. Hydrogen atom positions were not included on this toluene.

5.2. $\{K(C_7H_8)_2\}\{ZrCl_2[N(C_6F_5)_2]_3\}$ (**2**)

A lattice toluene was found and refined with isotropic thermal parameters, and without hydrogen atom positions. One of the toluene molecules bound to the potassium ion was disordered, and the methyl group was refined in three positions of one-third occupancy each (C50A, C50B, and C50C). All toluene molecules were restrained to approximate ideal geometry.

Table 6
Crystallographic data [a]

Compound	**1**·toluene	**2**·toluene	**3**·toluene	**4**	**5**·toluene
Formula	$C_{63}H_{16}F_{40}N_4NaO_2Ti$	$C_{57}H_{24}Cl_2F_{30}KN_3Zr$	$C_{86}H_{16}Cl_2F_{60}K_2N_6V_2$	$C_{32}H_{16}F_{20}FeN_2O_2$	$C_{41}H_{18}CoF_{20}N_2$
MW	1691.69	1522.01	2524.03	896.32	1005.52
Temperature (K)	203(2)	203(2)	203(2)	203(2)	203(2)
Crystal system	monoclinic	monoclinic	triclinic	monoclinic	triclinic
Space group	$C2/c$	$P2_1/c$	$P\bar{1}$	$C2/c$	$P\bar{1}$
a (Å)	22.3959(14)	19.3262(9)	12.2562(6)	21.2537(14)	11.8576(8)
b (Å)	14.9107(10)	16.5456(8)	15.3323(7)	10.9811(7)	12.3743(8)
c (Å)	20.0870(13)	18.8875(9)	24.3529(12)	16.254(1)	14.600(1)
α (°)	90	90	104.708(1)	90	69.639(1)
β (°)	112.123(2)	103.129(1)	91.890(1)	124.853(1)	83.229(1)
γ (°)	90	90	90.659(1)	90	81.941(1)
V (Å^3)	6214.0(7)	5881.7(5)	4423.0(4)	3113.0(3)	1983.1(2)
Z	4	4	2	4	2
D_{calc} (g ml^{-1})	1.808	1.719	1.895	1.912	1.684
Absorption coefficient (mm^{-1})	0.316	0.486	0.545	0.643	0.565
$F(000)$	3324	3000	2464	1776	998
θ Range (°)	2.20–26.43	1.66–25.35	1.66–25.03	2.2–26.4	1.5–26.4
Total reflections	27 321	27 821	16 090	14 156	8865
Independent reflections	6136 [$R_{int} = 0.053$]	10 592 [$R_{int} = 0.0234$]	14 184 [$R_{int} = 0.0305$]	3029 [$R_{int} = 0.0273$]	6882 [$R_{int} = 0.0225$]
Goodness-of-fit	1.112	1.603	0.964	1.413	1.160
Final R indices	$R_1 = 0.0788$	$R_1 = 0.0479$	$R_1 = 0.0503$	$R_1 = 0.0404$	$R_1 = 0.0576$
$[I > 2\sigma(I)]$	$wR_2 = 0.1272$	$wR_2 = 0.1449$	$wR_2 = 0.1209$	$wR_2 = 0.1116$	$wR_2 = 0.1399$

[a] $R_1 = \Sigma||F_o|-|F_c||/\Sigma|F_o|$ and $R_{2w} = [\Sigma[w(F_o^2-F_c^2)^2]/\Sigma[w(F_o^2)^2]]^{1/2}$; $w = 1/[\sigma^2(F_o^2)+(aP)^2]$, where $a = 0.0292$, 0.0630, 0.0713, 0.0557 and 0.0692 for compounds **1**–**5**, respectively.

5.3. $K\{VCl[N(C_6F_5)_2]_3\}$ (3)

The electron density of a disordered toluene molecule was removed from the unit cell using PLATON/SQUEEZE [85]. This resulted in two toluene molecules per cell being removed (298 e$^-$ per cell and 748 Å^3).

6. Supplementary material

Crystallographic data for the structural analyses have been deposited with the Cambridge Crystallographic Data Centre, CCDC No. 188730 for compound **1**, No. 188731 for compound **2**, No. 188732 for compound **3**, No. 188733 for compound **4** and No. 188734 for compound **5**. Copies of this information may be obtained free of charge from The Director, CCDC, 12 Union Road, Cambridge, CB2 1EZ, UK (fax: +44-1223-336033; e-mail: deposit@ccdc.cam.ac.uk or www: http://www.ccdc.cam.ac.uk).

Acknowledgements

This work was performed under the auspices of the Laboratory Directed Research and Development Program at Los Alamos National Laboratory. Los Alamos National Laboratory is operated by the University of California for the US Department of Energy under Contract W-7405-ENG-36.

References

[1] R. Kempe, Angew. Chem., Int. Ed. Engl. 39 (2000) 468.
[2] L.H. Gade, Chem. Commun. (2000) 173.
[3] G.J.P. Britovsek, V.C. Gibson, D.F. Wass, Angew. Chem., Int. Ed. Engl. 38 (1999) 428.
[4] F.T. Edelmann, Angew. Chem., Int. Ed. Engl. 34 (1995) 2466.
[5] J.D. Scollard, D.H. McConville, N.C. Payne, J.J. Vittal, Macromolecules 29 (1996) 5241.
[6] J.D. Scollard, D.H. McConville, J. Am. Chem. Soc. 118 (1996) 10008.
[7] R. Baumann, W.M. Davis, R.R. Schrock, J. Am. Chem. Soc. 119 (1997) 3830.
[8] L.C. Liang, R.R. Schrock, W.M. Davis, D.H. McConville, J. Am. Chem. Soc. 121 (1999) 5797.
[9] A.D. Horton, J. DeWith, A.J. VanderLinden, H. VandeWeg, Organometallics 15 (1996) 2672.
[10] F.G.N. Cloke, T.J. Geldbach, P.B. Hitchcock, J.B. Love, J. Organomet. Chem. 506 (1996) 343.
[11] F. Guerin, D.H. McConville, J.J. Vittal, Organometallics 15 (1996) 5586.
[12] A.R. Johnson, W.M. Davis, C.C. Cummins, S. Serron, S.P. Nolan, D.G. Musaev, K. Morokuma, J. Am. Chem. Soc. 120 (1998) 2071.
[13] C.E. Laplaza, M.J.A. Johnson, J.C. Peters, A.L. Odom, E. Kim, C.C. Cummins, G.N. George, I.J. Pickering, J. Am. Chem. Soc. 118 (1996) 8623.
[14] F.V. Cochran, P.J. Bonitatebus, R.R. Schrock, Organometallics 19 (2000) 2414.
[15] G.E. Greco, P.B. O'Donoghue, S.W. Seidel, W.M. Davis, R.R. Schrock, Organometallics 19 (2000) 1132.
[16] S.M. Reid, N. Beuner, R.R. Schrock, W.M. Davis, Organometallics 17 (1998) 4077.
[17] S.W. Seidel, R.R. Schrock, W.M. Davis, Organometallics 17 (1998) 1058.

[18] C. Rosenberger, R.R. Schrock, W.M. Davis, Inorg. Chem. 36 (1997) 123.
[19] K. Nomura, R.R. Schrock, W.M. Davis, Inorg. Chem. 35 (1996) 3695.
[20] R.R. Schrock, C.C. Cummins, T. Wilhelm, S. Lin, S.M. Reid, M. Kol, W.M. Davis, Organometallics 15 (1996) 1470.
[21] B. Neuner, R.R. Schrock, Organometallics 15 (1996) 5.
[22] R. Koppang, Acta Chem. Scand. 25 (1971) 3067.
[23] I.A. Koppel, R.W. Taft, F. Anvia, S.Z. Zhu, L.Q. Hu, K.S. Sung, D.D. Desmarteau, L.M. Yagupolskii, Y.L. Yagupolskii, N.V. Ignatev, N.V. Kondratenko, A.Y. Volkonskii, V.M. Vlasov, R. Notario, P.C. Maria, J. Am. Chem. Soc. 116 (1994) 3047.
[24] I. Koppel, J. Koppel, P.C. Maria, J.F. Gal, R. Notario, V.M. Vlasov, R.W. Taft, Int. J. Mass Spectrom. 175 (1998) 61.
[25] J.G. Watkin, D.R. Click, PCT Int. Appl. WO 9845039 A1, (1998) 86.
[26] D.R. Click, B.L. Scott, J.G. Watkin, Chem. Commun. (1999) 633.
[27] M.A. Putzer, B. Neumueller, K. Dehnicke, Z. Anorg. Allg. Chem. 624 (1998) 929.
[28] H.O. Frohlich, S. Keiser, Z. Chem. 14 (1974) 486.
[29] J.I. Song, P. Berno, S. Gambarotta, J. Am. Chem. Soc. 116 (1994) 6927.
[30] H.O. Frohlich, W. Romhild, Z. Chem. 20 (1980) 154.
[31] H.O. Frohlich, H. Kacholdt, Z. Chem. 15 (1975) 365.
[32] H.O. Frohlich, H. Kacholdt, Z. Chem. 15 (1975) 364.
[33] H.O. Frohlich, Z. Chem. 20 (1980) 108.
[34] M.M. Olmstead, P.P. Power, S.C. Shoner, Inorg. Chem. 30 (1991) 2547.
[35] H. Hope, M.M. Olmstead, B.D. Murray, P.P. Power, J. Am. Chem. Soc. 107 (1985) 712.
[36] V. Brito, H.O. Frohlich, B. Muller, Z. Chem. 19 (1979) 28.
[37] A. Spannenberg, A. Tillack, P. Arndt, R. Kirmse, R. Kempe, Polyhedron 17 (1998) 845.
[38] M.A. Putzer, B. Neumuller, K. Dehnicke, Z. Anorg. Allg. Chem. 624 (1998) 57.
[39] M.A. Putzer, M. Neumuller, K. Dehnicke, Z. Anorg. Allg. Chem. 624 (1998) 1087.
[40] R.K. Minhas, L. Scoles, S. Wong, S. Gambarotta, Organometallics 15 (1996) 1113.
[41] H. Plenio, Chem. Rev. 97 (1997) 3363.
[42] G.K. Fukin, S.V. Lindeman, J.K. Kochi, J. Am. Chem. Soc. 124 (2002) 8329.
[43] G.W. Gokel, S.L.S. Wall, E.S. Meadows, Eur. J. Org. Chem. 17 (2000) 2976.
[44] J.C. Ma, D.A. Dougherty, Chem. Rev. 97 (1997) 1303.
[45] D. Feller, D.A. Dixon, J.B. Nicholas, J. Phys. Chem. A 104 (2000) 11414.
[46] J.C. Amicangelo, P.B. Armentrout, J. Phys. Chem. A 104 (2000) 11420.
[47] D.L. Clark, R.V. Hollis, B.L. Scott, J.G. Watkin, Inorg. Chem. 35 (1996) 667.
[48] X.M. Yang, C.L. Stern, T.J. Marks, Angew. Chem., Int. Ed. Engl. 31 (1992) 1375.
[49] X.M. Yang, C.L. Stern, T.J. Marks, J. Am. Chem. Soc. 116 (1994) 10015.
[50] B. Findeis, M. Schubart, L.H. Gade, F. Moller, I. Scowen, M. McPartlin, Dalton Trans. (1996) 125.
[51] H. Memmler, U. Kauper, L.H. Gade, I.J. Scowen, M. McPartlin, Chem. Commun. (1996) 1751.
[52] J. Karl, G. Erker, R. Frohlich, J. Am. Chem. Soc. 119 (1997) 11165.
[53] Y.M. Sun, R.E.V.H. Spence, W.E. Piers, M. Parvez, G.P.A. Yap, J. Am. Chem. Soc. 119 (1997) 5132.
[54] C. Morton, I.J. Munslow, C.J. Sanders, N.W. Alcock, P. Scott, Organometallics 18 (1999) 4608.
[55] L.E. Sutton (Ed.), Tables of Interatomic Distances and Configuration in Molecules and Ions, Supplement 1956–1959 (Special publication No. 18), Chemical Society, London, UK, 1965.
[56] C.J. Schaverien, J.B.V. Mechelen, Organometallics 10 (1991) 1704.
[57] H.J. Gosink, F. Nief, L. Richard, F. Mathey, Inorg. Chem. 34 (1995) 1306.
[58] M.A. Beswick, N. Choi, A.D. Hopkins, M. McPartlin, M.A. Paver, D.S. Wright, Chem. Commun. (1998) 261.
[59] P.B. Hitchcock, J. Hu, M.F. Lappert, S. Tian, J. Organomet. Chem. 536 (1997) 473.
[60] C.P. Gerlach, J. Arnold, Dalton Trans. (1997) 4795.
[61] J.I. Song, S. Gambarotta, Chem. Eur. J. 2 (1996) 1258.
[62] P. Berno, S. Gambarotta, Organometallics 13 (1994) 2569.
[63] C.P. Gerlach, J. Arnold, Organometallics 16 (1997) 5148.
[64] W.K. Kim, M.J. Fevola, L.M. Liable-Sands, A.L. Rheingold, K.H. Theopold, Organometallics 17 (1998) 4541.
[65] A.T. Vlahos, T.A. Kabanos, C.P. Raptopoulou, A. Terzis, Chem. Commun. (1997) 269.
[66] V.C. Gibson, C. Redshaw, L.J. Sequeira, K.B. Dillon, W. Clegg, M.R.J. Elsegood, Chem. Commun. (1996) 2151.
[67] W. Czado, M. Maurer, U. Muller, Z. Anorg. Allg. Chem. 624 (1998) 1871.
[68] R.A. Bartlett, J.J. Ellison, P.P. Power, S.C. Shoner, Inorg. Chem. 30 (1991) 2888.
[69] R.A. Bartlett, P.P. Power, J. Am. Chem. Soc. 109 (1987) 7563.
[70] R.A. Andersen, K. Faegri, J.C. Green, A. Haaland, M.F. Lappert, W.P. Leung, K. Rypdal, Inorg. Chem. 27 (1988) 1782.
[71] M. Giusti, E. Solari, L. Gianninni, C. Floriani, A. Chiesi, A. Villa, C. Rizzoli, Organometallics 16 (1997) 5610.
[72] D.W. Lee, S.J. Lippard, J. Am. Chem. Soc. 120 (1998) 12153.
[73] K. Shelly, T. Bartczak, W.R. Scheidt, C.A. Reed, Inorg. Chem. 24 (1985) 4325.
[74] R.T. Boere, W.M. Brown, D.W. Stephan, C.J. Willis, Inorg. Chem. 24 (1985) 593.
[75] B.D. Murray, P.P. Power, Inorg. Chem. 23 (1984) 4584.
[76] R.A.J. Driessen, F.B. Hulsbergen, W.J. Vermin, J. Reedijk, Inorg. Chem. 21 (1982) 3594.
[77] J.S. Thompson, T. Sorrell, T.J. Marks, J.A. Ibers, J. Am. Chem. Soc. 101 (1979) 4193.
[78] F.A. Cotton, L.M. Daniels, G.T. Jordan, C.A. Murrilo, J. Am. Chem. Soc. 119 (1997) 10377.
[79] L.E. Manzer, Inorg. Synth. 21 (1982) 135.
[80] G.M. Sheldrick, SMART Version 4.210, Bruker Analytical X-ray Systems, Madison, WI, 1996.
[81] G.M. Sheldrick, SAINT Version 5.050, Bruker Analytical X-ray Systems, Madison, WI, 1998.
[82] G.M. Sheldrick, SADABS, first release; University of Gottingen, Germany.
[83] $R_1 = \Sigma||F_o| - |F_c||/\Sigma|F_o|$ and $R_2w = [\Sigma[w(F_o^2 - F_c^2)2]/\Sigma[w(F_o^2)^2]]1/2$; $w = 1/[\sigma^2(F_o^2) + (aP)^2]$, where $a = 0.0292, 0.0630, 0.0713, 0.0557$ and 0.0692.
[84] SHELXTL NT Version 5.10, Bruker Analytical X-ray Instruments, Madison, WI, 1997.
[85] A.L. Spek, Acta Crystallogr., Sect. A 46 (1990) C34.